

On the mechanism determining the transition mode from dropwise to film condensation

YOSHIO UTAKA and AKIO SAITO

Department of Mechanical Engineering, Tokyo Institute of Technology,
2-12-1 Ookayama, Meguro, Tokyo 152, Japan

and

HIROYUKI YANAGIDA

Kao Co., Tochigi, Japan

(Received 15 April 1987 and in final form 14 October 1987)

Abstract—Different modes of transition from dropwise to film condensation were investigated analytically and experimentally. Two types of transition modes, the continuous and jump modes, were observed. The dominant mechanism of heat transfer was discussed and the controlling factors were analyzed. A close agreement between the measurement and the analysis was obtained. It was confirmed that the modes of transition were determined by the gradient of the condensation curve on the bilogarithmic coordinates and by the ratio of the vapor-side heat transfer coefficient to the overall cooling-side conductance.

INTRODUCTION

WHEN THE surface subcooling is increased slowly enough so as to retain a steady state during the condensation of vapor on a lyophobic surface, the heat flux reaches its maximum value and then moves into a negative gradient region in which the heat flux decreases with the increase of surface subcooling. The aspect of condensation shifts from a dropwise mode to a film mode. By examining the previous results, the modes of transition can be classified into two types, i.e. the continuous transition [1-3] and the jump transition [3-5] in which the condensate film grows suddenly over the dropwise region and the whole condensing surface gets covered with liquid film. The jump phenomenon, however, has not yet been investigated thoroughly and the decisive mechanism remains unknown. The curve which shows the change of heat flux vs surface subcooling, called the condensation curve, is drawn by a solid line for the continuous transition mode as shown in Fig. 1(a). On the other hand, the condensation curve for the jump mode as shown in Fig. 1(b) is discontinuous. The unconnected portion (from point C to D in Fig. 1(b)) does not exist under steady state conditions because of the rapid growth of the liquid film. The jump is accompanied by a rapid decrease of the heat flux near the maximum heat flux point even though the cooling intensity hardly increases. If the entire aspect of dropwise condensation is to be understood, such a difference in the mode of transition needs to be brought to the attention of the investigators. The object of the present study is to clarify the mechanism determining the drop-to-film transition modes described above.

Stylianou and Rose [4] proposed two hypotheses

for the transition mechanism based on the microscopic drop behavior. They determined the values of parameters controlling the criteria of transition from their experimental results for ethylene glycol vapor and from the results by Tanasawa and Utaka [5] for steam. They stated that the transition modes described above depend on the distribution of nucleation sites on the surface. In the previous report [6] by the present authors, these hypotheses were examined using the experimental data for three organic vapors, i.e. propylene glycol, ethylene glycol and glycerol, on the copper surface promoted with tri-lauryl tri-thiophosphate [(C₁₂H₂₅S)₃P]. It was found difficult to specify the conditions of continuous transition and jump transition by the parameters of the proposed hypotheses.

A study has been made in this report on the transition modes from a completely different viewpoint that the transition is due to an instability of the overall heat transfer system including the vapor side, the heat transfer block and the cooling side.

CONSIDERATION OF INSTABILITY IN THE REGION OF NEGATIVE HEAT FLUX GRADIENT

The condensation curve shown in Fig. 1 can be divided into two domains according to the instability characteristics, i.e. the positive gradient region and the negative gradient region. In the positive gradient region, that is, from zero surface subcooling to point B and from point D to the larger subcooling, the cooling intensity must be increased in order to shift a point on the curve to the right. In the negative gradient

NOMENCLATURE

A	critical parameter for instability, equation (7)	T	temperature [K]
C	overall cooling-side conductance, $1/(1/C_b + 1/C_s + 1/C_c)$ [$\text{W m}^{-2} \text{K}^{-1}$]	T_c	coolant temperature [K]
C_b	conductance of heat transfer block [$\text{W m}^{-2} \text{K}^{-1}$]	T_s	condensing surface temperature [K]
C_c	cooling-side conductance [$\text{W m}^{-2} \text{K}^{-1}$]	T_v	vapor saturation temperature [K]
C_s	conductance of surface coating layer [$\text{W m}^{-2} \text{K}^{-1}$]	T_1	block temperature 2 mm from the condensing surface [K]
h	heat transfer coefficient of condensation, $q/\Delta T$ [$\text{W m}^{-2} \text{K}^{-1}$]	ΔT	condensing surface subcooling, $T_v - T_s$ [K]
q	heat flux [W m^{-2}]	ΔT_t	overall temperature difference, $T_v - T_c$ [K]
q_t	tentative heat flux (Fig. 2) [W m^{-2}]	ΔT^*	$\log \Delta T$
q^*	$\log q$	U	overall heat transfer coefficient, $1/(1/h + 1/C)$ [$\text{W m}^{-2} \text{K}^{-1}$].
q_t^*	$\log q_t$		
R	conductance ratio, h/C		
		Greek symbol	
		τ	time [s].

region, that is, from point B to D, the cooling intensity does not necessarily have to be increased to shift a point on the curve to the larger subcooling. The subject discussed in this chapter is to clarify the stability criteria under the increase of cooling intensity.

A one-dimensional overall heat transfer system as

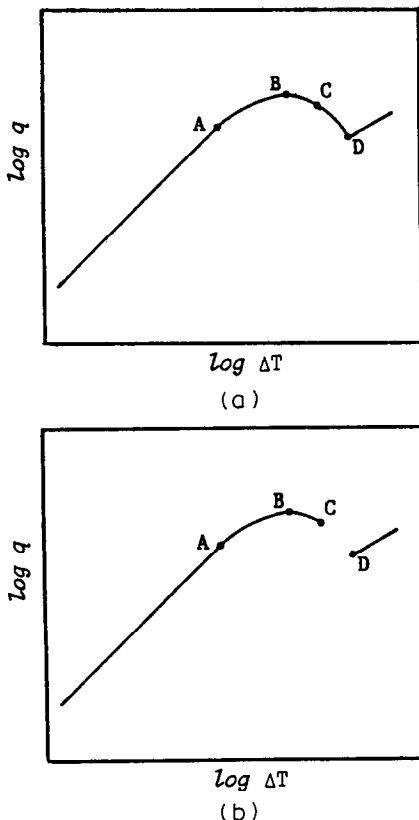


FIG. 1. Two transition modes from dropwise to film condensation: (a) continuous mode; (b) jump mode.

shown in Fig. 2(a) is considered. The vapor, the saturation temperature of which is T_v , condenses on one end of the surface of the heat transfer block with the heat transfer coefficient h . The surface temperature of the condensing surface is denoted as T_s . The surface of the other end is cooled by the coolant with the conductance C_c and the temperature T_c . Here, the conductance of the additional substance coating the cooling side is also contained in C_c . The conductances of the heat transfer block and the surface coating layer for achieving dropwise condensation are denoted as C_b and C_s , respectively, and the heat flux passing through the block as q . A study is made of the case when the point $(\Delta T, q)$ on the negative gradient curve, where ΔT denotes the vapor-to-surface temperature difference, shifts to the point $(\Delta T + d(\Delta T), q + dq)$ on the same condensation curve as depicted in Fig. 2(b). At the same time the heat transfer coefficient is changed from h to $h + dh$ when the cooling intensity monotonously increases realizing a quasi-steady state. Here, a tentative heat flux $q_t + dq_t$, defined as equation (4), is introduced to determine the criteria of instability by comparing the cooling intensity of the tentative heat flux $q_t + dq_t$ with the cooling intensity required to realize the real heat flux $q + dq$. In $q_t + dq_t$, the condensation heat transfer coefficient is $h + dh$ at the subcooling $\Delta T + d(\Delta T)$ and the values of other variables, i.e. C_b , C_c , C_s and ΔT_t , remain unchanged from those at subcooling ΔT , where q_t is equivalent to q at subcooling ΔT .

If an inequality

$$q + dq > q_t + dq_t \quad (1)$$

is satisfied, the cooling intensity must increase in order to shift the point $(\Delta T, q)$ to the point $(\Delta T + d(\Delta T), q + dq)$ on the curve because the real value of heat flux $q + dq$ is realized by augmenting the tentative heat flux $q_t + dq_t$. Under the condition expressed by

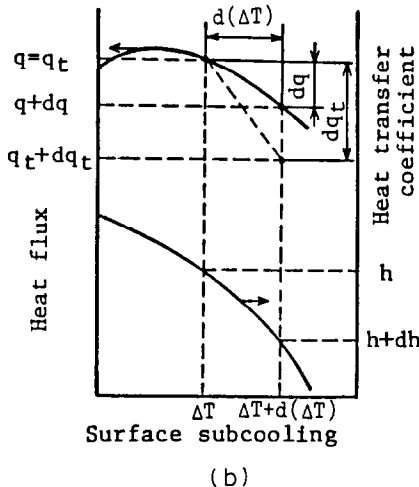
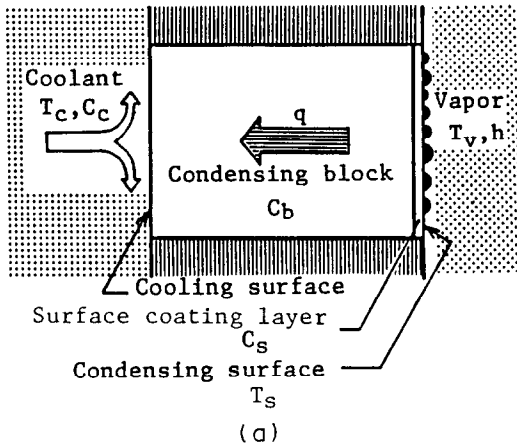


FIG. 2. Physical model: (a) overall heat transfer system; (b) condensation curve.

equation (1), a steady state is realized stably at the point $(\Delta T+d(\Delta T), q+dq)$.

If, on the contrary, an inequality

$$q+dq < q_t+dq_t \quad (2)$$

is satisfied, the cooling intensity must decrease, meaning the reduction of tentative heat flux in order to shift the point $(\Delta T, q)$ to $(\Delta T+d(\Delta T), q+dq)$ on the curve. Therefore, when the cooling intensity increases, the point $(\Delta T+d(\Delta T), q+dq)$ cannot exist stably under a steady state but is skipped causing the jump.

The critical parameter A determining the instability is introduced for quantitative discussions. Equations (3)–(5) hold for the system shown in Fig. 2(a)

$$q = q_t = U\Delta T_t = (1/h + 1/C)^{-1}\Delta T_t \quad (3)$$

$$q_t + dq_t = (1/(h+dh) + 1/C)^{-1}\Delta T_t \quad (4)$$

$$q + dq = (h+dh)(\Delta T + d(\Delta T)) \quad (5)$$

where

$$C = 1/(1/C_b + 1/C_s + 1/C_c)$$

is called the overall cooling-side conductance. Here,

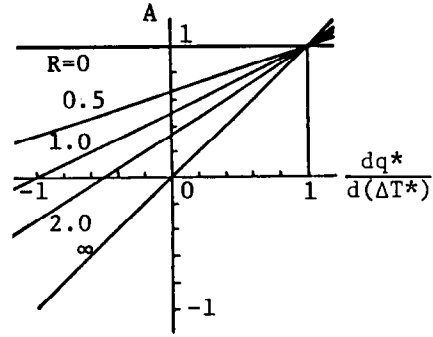


FIG. 3. Effect of R on A .

the increase of cooling intensity means the increase of $q_t + dq_t$ by changing C or ΔT_t in equation (4).

From equations (3)–(5), the tentative heat flux is expressed as follows taking logarithmic values of q and ΔT

$$\frac{d(\log q_t)}{d(\log \Delta T)} = \left\{ \frac{d(\log q)}{d(\log \Delta T)} - 1 \right\} / \left(\frac{h}{C} + 1 \right). \quad (6)$$

Using equation (6), the critical parameter, which determines whether the condensation curve exists stably or not as a steady state when the surface subcooling increases monotonously, is defined as follows:

$$A = \frac{dq^*}{d(\Delta T^*)} - \frac{dq_t^*}{d(\Delta T^*)} = \frac{1}{R+1} \left\{ R \frac{dq^*}{d(\Delta T^*)} + 1 \right\} \quad (7)$$

where $q^* = \log q$, $q_t^* = \log q_t$, $\Delta T^* = \log \Delta T$ and $R = h/C$. The value of A is determined only by the heat flux gradient $dq^*/d(\Delta T^*)$ of the condensation curve and the ratio R of the condensation heat transfer coefficient h and the overall cooling-side conductance C . Just as in equations (2) and (3), the instability condition is determined as follows:

$$\left. \begin{array}{l} A > 0, \quad \text{stable} \\ A < 0, \quad \text{unstable.} \end{array} \right\} \quad (8)$$

Figure 3 shows a change of A against $dq^*/d(\Delta T^*)$ due to the parametric variation of R . All the points on the condensation curve in the entire subcooling range are stable and are expressed as a continuous curve when $R \rightarrow 0$ ($C \rightarrow \infty$ or $h \rightarrow 0$). On the contrary, when R reaches infinity ($C \rightarrow 0$ or $h \rightarrow \infty$), the negative heat flux gradient region becomes unstable and cannot exist as a steady state. Since the actual cases exist between these two extremes, both the stable and unstable conditions appear depending on R and $dq^*/d(\Delta T^*)$.

EXPERIMENTAL APPARATUS AND PROCEDURES

The experimental apparatus is almost the same as that given in ref. [3], only the main items and the

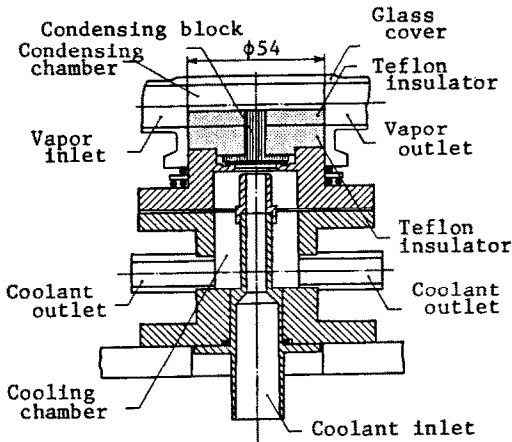


FIG. 4. Condensation apparatus.

improvements are highlighted here. A cross-sectional view of the condensing apparatus is shown in Fig. 4. The condensing surface was one end of a cylindrical copper block 8 mm in diameter. The vapor flowed through a rectangular duct 18 mm wide. One side of this duct was the surface of the condensing block and its ptfе insulator. The opposite side was a glass cover and the remaining two sides were fixed ptfе walls. The other end surface of the condensing block was cooled by a coolant jet and the vapor condensed on the condensing surface. The whole apparatus was made leak tight and the pressure and the flow rate of vapor could be kept at prescribed constant values. Propylene glycol was used for the condensing vapor. The coolants flowed from constant temperature baths. Oil, water and ethanol cooled by liquid nitrogen were used as coolants for a wide range of coolant temperature, and the velocity of coolant was regulated by using a bypass for varying the overall cooling-side conductance C . Moreover, to reduce C , a thin rubber (0.5 mm thick) with slightly higher thermal conductivity compared with the ordinary one was attached to the cooling surface. Constantan wires 0.1 mm in diameter insulated by glass tubes were soldered at the center of five holes 0.5 mm in diameter, each drilled 2 mm apart in the condensing block parallel to the condensing surface and a copper wire was soldered at the lower position on the side of the block. The heat flux and the surface temperature were obtained from these thermocouple e.m.f.s and the distances from the condensing surface of thermocouple junctions, assuming one-dimensional heat conduction. A thermocouple placed in front of the condensing surface in the vapor duct measured the vapor temperature and another one at the entrance of the coolant jet measured the coolant temperature to obtain the overall temperature difference. The same copper block was used throughout the experiment. First, it was coated with ptfе. Then, after removing the ptfе layer, trilauryl triphosphite was adsorbed. Hence, two different kinds of condensing surface were used. The vapor

superheat and the conductance of the ptfе layer were determined by the method described in ref. [2].

Quasi-steady-state measurement was carried out not only to obtain the condensation curve under the constant vapor condition but also to identify the jump point precisely, that is, the coolant temperature was lowered very slowly to realize the state close enough to the steady state while keeping the pressure and the flow rate of the vapor in the experimental system constant. The thermocouple e.m.f.s were recorded and then the condensation curve was drawn.

DETERMINATION OF A

The value of A was determined from the measured results.

(1) The heat flux q , the surface subcooling ΔT and the overall temperature difference ΔT_i were determined from the vapor saturation temperature T_v , the coolant temperature T_c and the temperatures obtained from the e.m.f.s of thermocouples in the condensing block.

(2) By fitting the curves obtained by the least square method, the relations between q^* and $\Delta T^*(q^*(\Delta T^*))$, and between ΔT_i and $\Delta T(\Delta T_i(\Delta T))$ were determined.

(3) The value of C was obtained from equation (3) using q , h and $\Delta T_i(\Delta T)$, and the value of A was determined by R and $dq^*/d(\Delta T^*)$ over the whole subcooling range of the condensation curve.

RESULTS AND DISCUSSIONS

Figures 5 and 6 show the results for the ptfе-coated surface under nearly the same vapor-side conditions with different overall cooling-side conductance C . The result for relatively large C utilizing the water jet cooling is shown in Fig. 5(a). The continuous condensation curve was obtained and the open circles and the solid line denote the measured values and the fitted curve, respectively. The value of A shown in Fig. 5(b) was calculated from the method described in the previous section using $q^*(\Delta T^*)$ and $\Delta T_i(\Delta T)$ shown in Figs. 5(a) and (c), respectively. The value of A first decreases, reaches a minimum value and then increases as ΔT increases. The value of A remains positive throughout the entire subcooling region. This means that the whole region exists stably as a steady state according to equation (8), and it is in good agreement with the measured result.

Figure 6(a) shows the results of the measurement which was undertaken for the reduced value of C by attaching a relatively high-conductive rubber to the cooling surface as a thermal resistant material. Ethanol near its melting point cooled by liquid nitrogen was used as the coolant because a large overall temperature difference was needed. In this experiment, the discontinuous curve with the jump from dropwise to film condensation was measured. The surface sub-

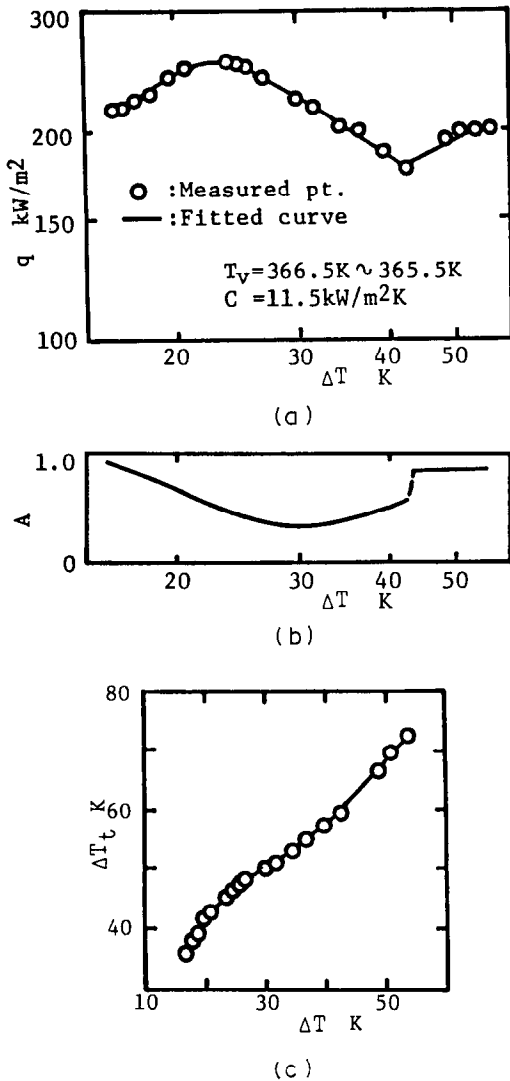


FIG. 5. Results on ptfе-coated surface [1]: (a) condensation curve; (b) value of A ; (c) ΔT_t vs ΔT .

cooling measured at the jump point was 21.7 K. The solid line denotes the fitted curve. It is seen from Fig. 6(b) that the value of A decreases monotonously with increasing ΔT and becomes negative in the subcooling range larger than 23.1 K. This value agrees quite well with the value at the measured jump point. The dotted line expresses the unstable region for which no data were available under a steady condition and A in this region was estimated by using the fitted curve shown in Fig. 6(a). The value of C at the jump point was used for the calculation in the skipped region because the jump region was passed through very quickly in contrast to the very slow decrease of coolant temperature in the measurement as described later. Since the vapor-side conditions were the same for both cases given in Figs. 5(a) and 6(a), the fitted curve at the jump region in Fig. 6(a) was determined in a similar manner to the curve in Fig. 5(a). The examples of measured temperature variations are shown in Fig.

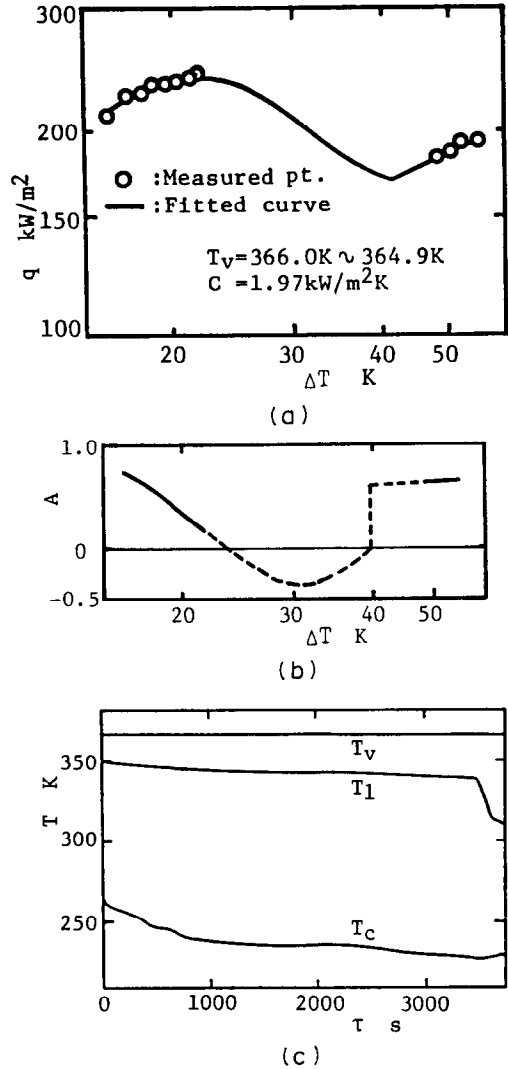


FIG. 6. Results on ptfе-coated surface [2]: (a) condensation curve; (b) value of A ; (c) temperature variations.

6(c). As the coolant temperature T_c was changed very slowly under a constant vapor saturation temperature T_v , a quasi-steady variation excluding the jump domain and the abrupt change at the jump region can be confirmed.

It is understood by comparing Figs. 5 and 6 that the continuous curve obtained with large C becomes discontinuous in the negative heat flux gradient region with the jump under conditions of small C .

Figure 7 gives the calculation results for the variations of A in the dropwise condensation region when the value of C alone was changed and $dq^*/d(\Delta T^*)$ and h were fixed at the measured values of the continuous curve shown in Fig. 5(a). The unstable regions of $A < 0$ expand with decreasing C . The variation of A for $C = 1.97 \text{ kW m}^{-2} \text{ K}^{-1}$ shown in Fig. 6(b) is similar to the calculation for $C = 2.0 \text{ kW m}^{-2} \text{ K}^{-1}$ given in Fig. 7. The effect of C described above is also confirmed with this result.

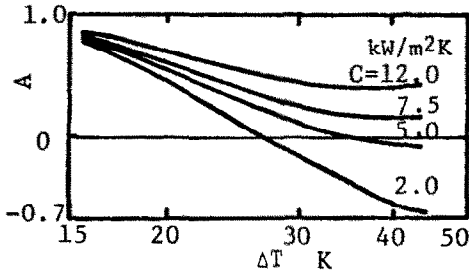


FIG. 7. Effect of overall cooling-side conductance.

Figures 8 and 9 show the results of the experiments and calculations using the copper surface promoted with trilauryl triphosphite for propylene glycol vapor. The ptfе layer used for the experiment shown in Figs. 5 and 6 was peeled off and trilauryl triphosphite was adsorbed directly on the copper condensing surface. In Figs. 8 and 9, $C_s = 0$ and all the conditions were the same except for the cooling medium. The values of C were different, i.e. the water jet cooling was Fig. 8 and the oil cooling was Fig. 9. The discontinuous curves showing the jumps were obtained for both results given in Figs. 8(a) and 9(a). The surface subcooling ΔT at the jump point for water cooling was 22.1 K and was slightly larger than that of 20.6 K for the oil cooling. The changes of vapor temperature T_v , the coolant temperature T_c and the temperature of the heat transfer block T_1 for the case shown in Fig. 9(b) are given in Fig. 9(c). It is confirmed that T_c decreased slowly while T_v was kept constant. The change in T_1 caused a jump to occur suddenly as shown in Fig. 6(c), with the jump domain divided in two stages. The jump point of the first stage

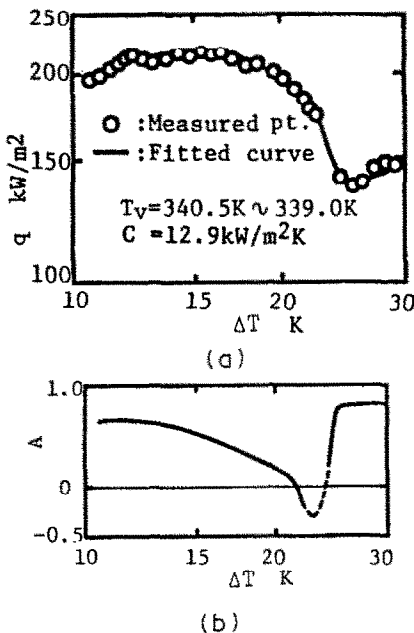
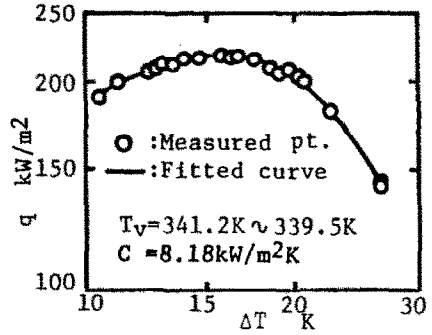
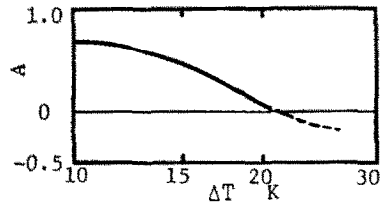


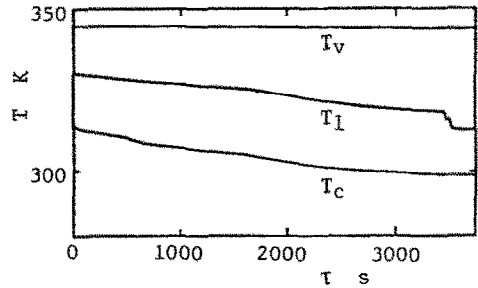
FIG. 8. Results on trilauryl triphosphite adsorbed copper surface [1]: (a) condensation curve; (b) value of A .



(a)



(b)



(c)

FIG. 9. Results on trilauryl triphosphite adsorbed copper surface [2]: (a) condensation curve; (b) value of A ; (c) temperature variations.

was adopted as a jump point here since ΔT of the second stage was very close to the first one. The values of ΔT where $A = 0$ were 21.7 and 21.0 K for both of the calculations as seen from the variation curves of A in Figs. 8(b) and 9(b) and are very close to the measured results of jump points.

The surface subcoolings of measurements at the jump points $(T_j)_m$ and of the calculations $(T_j)_c$ where $A = 0$ for all the results in this report and the results of the former report [2] containing ΔT_j measurements are summarized in Table I. The symbol — denotes that the continuous curve was obtained with no jump. The values of A were positive throughout the whole subcooling range under all conditions. For the results with the jumps, the average difference between $(T_j)_m$ and $(T_j)_c$ was very small at about 0.5 K showing a close agreement. Thus, it is understood that the jump from dropwise to film condensation is caused by the instability in the overall heat transfer system that is determined by the gradient of the heat flux against the surface subcooling on the bilogarithmic coordinates

Table 1. Comparison of measurements and calculations of jump point subcoolings

Vapor	Heat transfer surface (promoter)	Vapor temperature, T_v (K)	Subcooling at jump point		$(T_j)_m - (T_j)_c$	Overall cooling-side conductance ($\text{kW m}^{-2} \text{K}^{-1}$)	
			Meas. $(T_j)_m$ (K)	Cal. $(T_j)_c$ (K)			
Propylene glycol	ptfe-coated copper	365	—	—	—	11.5	Present work
		365	21.7	23.1	-1.4	1.97	
		363	—	—	—	13.7	Ref. [2]
		363	—	—	—	13.6	
		388	—	—	—	14.0	
	388	—	—	—	13.7		
	Copper (trilauryl trithiophosphate)	340	22.1	21.7	0.4	12.9	Present work
		340	20.6	21.0	-0.4	8.2	
		340	21.5	22.4	-0.9	12.9	
		353	12.8	14.1	-1.3	8.6	
353		13.7	12.7	1.0	10.6		
365	14.5	15.3	-0.8	16.6			

—, Continuous mode ($A > 0$).

and by the ratio of the vapor-side heat transfer coefficient to the overall cooling-side conductance. It can be predicted from the results described above that, with sufficiently large overall cooling-side conductance, the condensation curve will always be a single continuous one under all vapor conditions when the surface subcooling increases (the cooling intensity increases monotonously) and that it will often be a discontinuous one depending on the conditions of the overall heat transfer system.

CONCLUDING REMARKS

The heat transfer mechanism determining the two different modes of transition from dropwise to film condensation, i.e. the continuous mode and the jump mode was investigated analytically and experimentally. As a result, it was found that the transition modes were determined by the gradient of the condensation curve on the logarithmic scale, and the ratio of the condensation heat transfer coefficient to the overall cooling-side conductance. It was concluded that, although the condensation curve could exist as a continuous one with sufficient high overall cooling-side conductance, the unstable region which could not be found in a steady state appeared in a part of the

negative gradient region and the curve became discontinuous, depending on the thermal conductivity and the size of the heat transfer block and the cooling condition.

REFERENCES

1. T. Takeyama and S. Shimizu, On the transition of dropwise-film condensation, *Proc. 5th Int. Heat Transfer Conf.*, Vol. 3, pp. 274-278 (1974).
2. Y. Utaka, A. Saito, T. Tani, H. Shibuya and K. Katayama, Study on dropwise condensation curves (measurement of propylene glycol vapor on PTFE coated surface), *Bull. J.S.M.E.* **28**, 1150-1157 (1985).
3. Y. Utaka, A. Saito, H. Ishikawa and H. Yanagida, Study on dropwise condensation curves (dropwise to filmwise transition of propylene glycol, ethylene glycol and glycerol vapors on a copper surface using a monolayer type promoter (part 1)), *Bull. J.S.M.E.* **29**, 4228-4234 (1986).
4. S. A. Stylianou and J. W. Rose, Drop-to-filmwise condensation transition: heat transfer measurements for ethanediol, *Int. J. Heat Mass Transfer* **26**, 747-760 (1983).
5. I. Tanasawa and Y. Utaka, Measurement of condensation curves for dropwise condensation of steam at atmospheric pressure, *J. Heat Transfer* **105**, 633-638 (1983).
6. Y. Utaka, A. Saito, H. Ishikawa and H. Yanagida, Transition from dropwise condensation to film condensation of propylene glycol, ethylene glycol and glycerol vapors, *Proc. ASME-JSME Thermal Engng Joint Conf.*, Vol. 4, pp. 377-384 (1987).

SUR LE MECANISME DETERMINANT LA TRANSITION ENTRE LA CONDENSATION EN GOUTTES ET CELLE EN FILM

Résumé—On étudie analytiquement et expérimentalement différents modes de transition depuis la condensation en gouttes jusqu'à celle en film. On observe deux modes de transition, l'un continu et l'autre brusque. Le mécanisme dominant de transfert de chaleur est discuté et les facteurs déterminants sont analysés. Un accord satisfaisant est obtenu entre les mesures et la théorie. Il est confirmé que les modes de transition sont déterminés par le gradient de la courbe de condensation rapportée aux coordonnées logarithmiques et par le rapport du coefficient de transfert thermique du côté de la vapeur, à la conductance globale du côté du refroidissement.

ZUM ÜBERGANGS-MECHANISMUS ZWISCHEN TROPFEN- UND FILMKONDENSATION

Zusammenfassung—Es wurden unterschiedliche Arten des Übergangs von der Tropfen- zur Filmkondensation analytisch und experimentell untersucht. Zwei Typen von Übergangsarten, die kontinuierliche und die sprunghafte, wurden beobachtet. Der dominierende Wärmeübergangs-Mechanismus wurde diskutiert, die bestimmenden Faktoren analysiert. Die Übereinstimmung zwischen Experiment und Theorie ist gut. Es hat sich bestätigt, daß die Art des Übergangs von der Steigung der Kondensationskurve in doppel-logarithmischer Auftragung und vom Verhältnis des dampfseitigen Wärmeübergangskoeffizienten zur gesamten kühlseitigen Leitfähigkeit bestimmt wird.

О МЕХАНИЗМЕ, ОПРЕДЕЛЯЮЩЕМ РЕЖИМ ПЕРЕХОДА ОТ КАПЕЛЬНОЙ КОНДЕНСАЦИИ К ПЛЕНОЧНОЙ

Аннотация—Аналитически и экспериментально исследованы различные режимы перехода от капельной конденсации к пленочной: непрерывный и скачкообразный. Дается анализ доминирующего механизма теплопереноса и определяющих факторов. Получено хорошее соответствие между результатами измерений и данными анализа. Подтверждено, что режимы перехода определяются наклоном кривой конденсации в билогарифмических координатах и отношением коэффициента теплоотдачи со стороны пара к суммарному коэффициенту теплопроводности подложки.